J. Fluid Mech. (2000), *vol.* 408, *pp.* 179–204. Printed in the United Kingdom

Polynya flux model solutions incorporating a parameterization for the collection thickness of consolidated new ice

By NICHOLAS R. T. BIGGS, MIGUEL A. MORALES MAQUEDA† AND ANDREW J. WILLMOTT

Department of Mathematics, Keele University, Keele, Staffordshire, ST5 5BG, UK

(Received 30 April 1999 and in revised form 16 November 1999)

Previous polynya flux models have specified a constant value for the collection thickness of frazil ice, H, at the polynya edge. In certain circumstances, this approach can cause the frazil ice depth, h, within the polynya, to exceed H, a result which violates assumptions made in the formulation of the ice flux balance equations at the polynya edge. To overcome this problem, a parameterization for H is derived in terms of the depth of frazil ice arriving at the polynya edge and the component, normal to the polynya edge, of the frazil ice velocity relative to the velocity of the consolidated ice pack. Thus, H is coupled to the unknown polynya edge. Using the new parameterization for H, an analysis of the unsteady one-dimensional opening of a coastal polynya is presented. Analytical solutions are also derived, using the new parameterization for H, for steady-state two-dimensional polynyas adjacent to a semi-infinite and finite-length coastal barrier, the latter case representing a prototype island. In all cases, the solutions show close qualitative and quantitative agreement with those derived using a constant value for H. However, the steady-state two-dimensional polynya edge can, in certain circumstances, exhibit a corner at the point where the offshore equilibrium width is reached. Precise conditions for the existence of a corner are derived in terms of the orientation of the frazil ice velocity ($\boldsymbol{u}$) and the consolidated ice velocity ($\boldsymbol{U}$). Upper and lower bounds are also obtained for the area of the steady-state island polynya, and it is shown that over a large range of orientations of $\boldsymbol{u}$ and $\boldsymbol{U}$, the area exceeds that associated with the island polynya with constant H. Finally, two simulations of the St. Lawrence Island Polynya are presented using the new parameterization for H, and the results are compared with the H-constant theory.

1. Introduction

Wind-driven coastal polynyas are areas of near ice-free waters which form between the coast and the offshore consolidated ice pack in predictable, recurrent locations at times and under climatological conditions where we would expect the waters to be ice-covered. They arise as a consequence of offshore advection of frazil ice by the wind and surface ocean currents, creating what is called a latent heat polynya (Smith, Muench & Pease 1990). The horizontal extent of coastal polynyas can range from a

† Present address: Potsdam Institute for Climate Impact Research, P.O. Box 60 12 03, 14412 Potsdam, Germany.

few kilometres up to several hundred kilometres (e.g. the North Water Polynya in the Arctic). Coastal latent heat polynyas are ubiquitous features adjacent to the coast of Antarctica (Markus & Burns 1995), because of the persistent offshore katabatic winds. Upwelling of warm water can also contribute to the formation and maintenance of what is called a sensible heat polynya (Smith *et al.* 1990). Both sensible and latent heat mechanisms frequently operate in the maintenance of coastal polynyas (Darby, Willmott & Mysak 1994; Fichefet & Goosse 1998).

Frazil ice formed within the polynya 'piles up' in the form of consolidated new ice at the offshore edge of the polynya (Lebedev 1968; Pease 1987). The area of a polynya is determined by the frazil ice production within it and the offshore export of consolidated new ice. This observation is fundamental in the development of what are termed 'polynya flux models'. Unsteady one-dimensional polynya flux models were formulated by Pease (1987) and Ou (1988). The generalization of unsteady flux models to two dimensions is discussed by Morales Maqueda & Willmott (1999) and the references therein. Coastal polynyas around Antarctica are sites where deep water is produced (Gordon & Comiso 1988; Grumbine 1991). This deep water sinks and spreads to form part of the global thermohaline circulation. Coarse-resolution global ocean circulation models (OCMs) do not adequately resolve coastal polynyas, and as a consequence they do not correctly model the rate of deep water production which is crucial for a realistic model of the global thermohaline circulation. A method of overcoming this problem is to introduce into OCMs a parameterization of the surface buoyancy flux distribution within coastal polynyas. Two-dimensional polynya flux models offer a possible method for this parameterization.

In all polynya flux models to date, the collection thickness, H, of consolidated new ice at the edge is assumed to be constant. Clearly, H should be determined by the dynamics and thermodynamics of the polynya flux model. The purpose of this paper is to describe a method for doing this, and to then derive expressions for the spin-up time, alongshore adjustment length scale and area of coastal polynyas adjacent to a variety of simple coastline configurations. Naming a constant value for H in the unsteady two-dimensional flux model of Morales Maqueda & Willmott (1999) leads to a theory which is not completely robust, for when using this theory to determine the evolution of a two-dimensional polynya from one steady state to a new steady state, it is possible for the frazil ice depth at the polynya edge to exceed H, thereby violating the assumptions made in the derivation of the governing ice flux equations. To see this explicitly, note that in a steady-state polynya flux model, frazil ice on the verge of reaching the polynya edge can have grown to a depth which is comparable to, but which does not exceed, the consolidated new ice depth H. An impulsive change in the direction of the wind stress then causes both the frazil ice and consolidated new ice to alter their directions of drift. Thus, interior frazil ice now drifts towards a new evolving polynya edge. It is then possible for interior frazil ice to grow to a depth greater than H before it reaches the newly adjusting polynya edge. It should be stressed that this phenomenon is not common in flux models. However, it is clear that what is missing in the earlier flux model theories is a description of the physics which controls the conversion process of frazil ice to consolidated new ice.

The plan of the paper is as follows. In § 2, we present a new unified derivation of the one-dimensional flux theories of Pease (1987) and Ou (1988), which clarifies the relationship between the two studies. In this section we also derive a new parameterization for the frazil ice collection thickness H. Section 3 applies the parameterization for H to the one-dimensional unsteady problem, wherein a polynya opens in a direction perpendicular to a straight coastline; in § 4 we investigate the sensitivity of this solution to variations in the air temperature and offshore wind speed. In § 5 and § 6, we study solutions of the two-dimensional steady-state polynya flux model, with the new parameterization for H, for semi-infinite and finite-length straight coastal barriers, respectively. In § 6, we also present simulations of the St. Lawrence Island Polynya of the northern Bering Sea. Finally, in § 7, we present a summary of the results, and a discussion of future research problems in polynya modelling.

2. A parameterization for the collection thickness of consolidated new ice

We begin by placing the one-dimensional time-dependent flux theories of Pease (1987) and Ou (1988) in a unified context. Consider a one-dimensional polynya, and suppose for simplicity that it commences its growth at $t = 0$. We assume that the frazil ice production rate, F, the frazil ice velocity $\boldsymbol{u} = u\boldsymbol{i}$, and the consolidated new ice velocity $\boldsymbol{U} = U\boldsymbol{i}$ are all uniform, where $\boldsymbol{i}$ is a unit vector in the offshore direction. The net amount of ice produced within the polynya since it started to open must be equal to the total amount of frazil ice that has transformed into consolidated new ice, plus the amount of frazil ice remaining within the polynya. This conservation law for ice mass can be expressed as

$$\int_0^t FX\,\mathrm{d}t = \int_0^t H\left(U - \frac{\mathrm{d}X}{\mathrm{d}t}\right)\mathrm{d}t + V_f, \tag{2.1}$$

where $X(t)$ is the polynya width, H is the collection thickness for consolidated new ice at the polynya edge, and V_f is the volume of frazil ice, per alongshore unit length, within the polynya. Differentiating (2.1) with respect to time yields

$$FX = H\left(U - \frac{\mathrm{d}X}{\mathrm{d}t}\right) + \frac{\mathrm{d}V_f}{\mathrm{d}t}. \tag{2.2}$$

Pease (1987) assumes that no frazil ice exists within the polynya (i.e. $V_f = 0$), in which case (2.2) becomes

$$\frac{\mathrm{d}X}{\mathrm{d}t} = \frac{HU - FX}{H}. \tag{2.3}$$

In contrast, Ou (1988) considers a finite residence time for frazil ice within the polynya so that

$$V_f = \int_0^X h\,\mathrm{d}x, \tag{2.4}$$

where $h(x,t)$ is the frazil ice depth at a distance x from the coast at time t. From (2.4),

$$\frac{\mathrm{d}V_f}{\mathrm{d}t} = \int_0^X \frac{\partial h}{\partial t}\mathrm{d}x + \frac{\mathrm{d}X}{\mathrm{d}t}\,h(X,t). \tag{2.5}$$

Continuity of frazil ice mass is given by

$$\frac{\partial h}{\partial t} + \frac{\partial}{\partial x}(hu) = F,$$

which upon combining with (2.5) gives

$$\frac{\mathrm{d}V_f}{\mathrm{d}t} = \frac{\mathrm{d}X}{\mathrm{d}t}\,h(X,t) + FX - h(X,t)u, \tag{2.6}$$

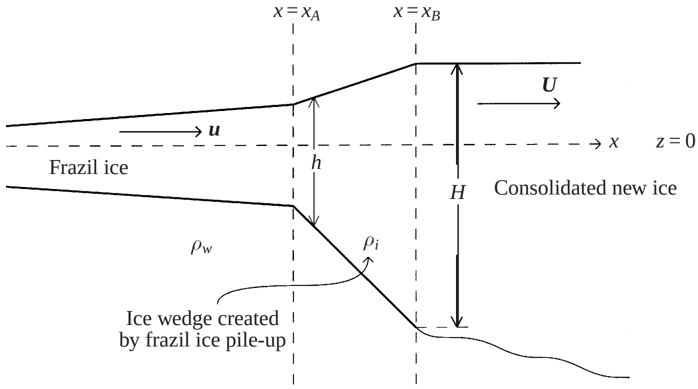

FIGURE 1. Schematic of the frazil ice wedge formed at the polynya edge.

where we have also assumed that the frazil ice depth at the coast, $h(0, t)$, is zero. Substituting (2.6) into (2.2) yields

$$\frac{\mathrm{d}X}{\mathrm{d}t} = \frac{HU - h(X,t)u}{H - h(X,t)}, \tag{2.7}$$

which is the equation derived by Ou (1988). In contrast with the above method, Ou (1988) exploits an ice flux balance across a control volume which is centred at the evolving polynya edge. However, the relationship between the Pease (1987) and Ou (1988) formulations of the problem becomes transparent in the derivation above.

Although the above derivation does not demand it, in both Pease (1987) and Ou (1988), H is assumed to be constant. Indeed, this assumption is carried over to the two-dimensional flux theory developed by Darby, Willmott & Somerville (1995), Willmott, Morales Maqueda & Darby (1997) and Morales Maqueda & Willmott (1999). In one-dimensional flux models with a coast at $x = 0$, we assume $h(0, t) = 0$, and therefore we expect $0 \leqslant h < H$ throughout the polynya. Clearly, if $h = H$, (2.7) becomes invalid. In practice, the pile-up of frazil ice at the polynya edge produces consolidated new ice of thickness H which is not constant.

To determine a collection law for H, we adopt the approach of Martin & Kauffman (1981) and Bauer & Martin (1983), in which the authors consider the pile-up of grease ice at the downwind edge of a lead. In contrast with polynyas, a lead is essentially a one-dimensional feature, although we might expect the physics controlling the pile-up of frazil ice to be the same as that controlling grease ice pile-up, as grease ice simply consists of a mixture of water and frazil ice platelets. Initially we will obtain a collection law for H in a one-dimensional polynya model, and then we will generalize it to two dimensions. Figure 1 shows a schematic diagram of frazil ice at a polynya edge. We consider a frame of reference in which the consolidated new ice is stationary, and following Bauer & Martin (1983) we determine H by demanding that the gradient of the vertically integrated momentum flux balances the ice set-up within this reference frame.

We suppose that there are two layers of fluid: an active upper layer of frazil ice with density ρ_i (assumed constant), and a lower layer of water of density ρ_w (also assumed constant). Assuming hydrostatic balance and neglecting temporal variations in the fluid velocities, our governing equations are

$$uu_x = -\frac{g}{\rho_w}(\rho_w - \rho_i)h_x, \quad (uh)_x = 0, \tag{2.8a,b}$$

where u is the vertically averaged frazil ice velocity, and h is the depth of the frazil ice layer.

The frazil ice commences the pile-up process at $x = x_A$, which is the point nearest to the offshore ice pack that the frazil ice can reach before its velocity is affected by the influence of the consolidated new ice. At $x = x_B$, the frazil ice depth is assumed equal to the consolidated new ice depth, H, so that $h|_{x=x_B} = H$. The distance $x_B - x_A$ is much smaller than the average polynya width (Martin & Kauffman 1981), so we define the point $x = x_A$ to be the polynya edge, but also refer to H as the frazil ice collection depth or consolidated new ice depth *at the polynya edge*. Integration of (2.8*a*) from $x = x_A$ to $x = x_B$ yields

$$\tfrac{1}{2}\{(u_B - U)^2 - (u_A - U)^2\} = -\frac{g}{\rho_w}(\rho_w - \rho_i)(h_B - h_A), \tag{2.9}$$

where U is the velocity of the consolidated ice pack, and subscripts denote the positions at which the variables are evaluated. Assuming that the momentum flux is brought to zero at the location of the maximum ice set-up (at $x = x_B$), (2.9) reduces to

$$\tfrac{1}{2}(u_A - U)^2 = \frac{g}{\rho_w}(\rho_w - \rho_i)(h_B - h_A), \tag{2.10}$$

whence use of the equality $h|_{x=x_B} = H$, gives

$$H = h_A + c(u_A - U)^2, \tag{2.11}$$

where $c = \rho_w/(2g(\rho_w - \rho_i))$. We adopt the values $\rho_i = 950\,\mathrm{kg\,m^{-3}}$ and $\rho_w = 1029\,\mathrm{kg\,m^{-3}}$ of Martin & Kauffman (1981) throughout the subsequent work, which gives $c \approx 0.665\,\mathrm{m^{-1}\,s^2}$. Notice that H depends on both polynya thermodynamics (via h_A), and the wind stress and wind generated currents (via u_A and U), and given these inputs, is completely determined.

An immediate generalization of (2.11) to the case of a two-dimensional polynya is

$$H = h_A + c|(\boldsymbol{u} - \boldsymbol{U}) \cdot \boldsymbol{n}|^2, \tag{2.12}$$

where $\boldsymbol{n}$ is the unit normal to the polynya edge (directed away from the polynya), and $\boldsymbol{u}$ now denotes the velocity of the frazil ice at the polynya edge. In this case, H is given in terms of only the component of the relative velocity $(\boldsymbol{u} - \boldsymbol{U})$ normal to the polynya edge, and the depth of the frazil ice reaching the polynya edge.

In the following sections of the paper we examine polynya flux solutions which satisfy (2.12). Notice that (2.12) now couples H to the unknown polynya edge through the normal vector $\boldsymbol{n}$. Thus, even when $\boldsymbol{u}$ and $\boldsymbol{U}$ are both assumed constant, the collection depth varies for a two-dimensional polynya because $\boldsymbol{n}$ varies in direction along the polynya edge. There are two major advantages of using the collection depth law (2.12). First, (2.12) contains only one parameter, c, the value of which is tightly constrained. Second, (2.12) ensures that $H > h_A$, in which case we would expect polynya flux models to be robust using this parameterization. What is not clear, *a priori*, is whether (2.12) introduces radically different polynya solutions compared with the case when H is constant.

3. The unsteady one-dimensional problem

We first examine the one-dimensional time-dependent problem, wherein a polynya opens in a direction perpendicular to a straight coast. Assume for simplicity that the polynya commences opening at $t = 0$. Then from (2.7), the position of the polynya edge at time $t > 0$ is determined by

$$\frac{\mathrm{d}X}{\mathrm{d}t} = \frac{HU - h_C u}{H - h_C} \tag{3.1}$$

for the polynya width $X(t)$, subject to the initial condition $X(0) = 0$. In (3.1), $h_C = h(X,t)$ denotes the frazil ice depth at the polynya edge.

We consider the case in which u and U are uniform, with $u > U > 0$, so that the polynya width has a finite upper bound. The frazil ice depth h in the polynya is found by integrating the one-dimensional frazil ice mass conservation equation

$$\frac{\partial h}{\partial t} + u\frac{\partial h}{\partial x} = F, \tag{3.2}$$

where F is the frazil ice production rate, subject to the coastal boundary condition $h(0,t) = 0$.

We consider an infinite straight coastline with the polynya occupying the region $x > 0$. The one-dimensional nature of the problem provides a corresponding simplification to the parameterization (2.12) of the consolidated ice depth H, because in this case the polynya edge is always parallel to the y-axis, and $\boldsymbol{n} = \boldsymbol{i}$. Thus H is here given by

$$H = h_C + c(u - U)^2. \tag{3.3}$$

For the case when F is constant, the solution of (3.2) subject to the coastal boundary condition is simply $h(x,t) = Fx/u$, in which case $h_C = FX/u$. Substituting this expression for h_C, and also (3.3) into (3.1), yields the differential equation

$$\frac{\mathrm{d}X}{\mathrm{d}t} = \frac{cu(u-U)U - FX}{cu(u-U)}. \tag{3.4}$$

We note that the form of this equation is superficially similar to the evolution equation of Pease (1987), namely (2.3), although it is to be stressed that this resemblance is coincidental. Pease (1987) assumes a frazil ice drift rate that is unbounded, and a constant value for the frazil ice collection depth H. In contrast, we assume that the rate of frazil ice drift, u, is finite, and that H varies and is given by (3.3). The physical ideas on which the polynya edge evolution equations (2.3) and (3.4) are based are thus fundamentally distinct.

Integrating (3.4) gives

$$X = L\{1 - \exp[-Ut/L]\}, \tag{3.5}$$

where

$$L = (cu/F)U(u - U) \tag{3.6}$$

is the steady-state or 'Lebedev–Pease' width associated with the new frazil ice collection depth law. Generally, the polynya steady-state width L can be determined from the requirement that the total frazil ice production within the polynya, FL, balances the consolidated new ice flux out of the polynya, $H|_L U$, where $H|_L$ denotes the consolidated ice-sheet thickness at the equilibrium width L. This gives $L = H|_L U/F$, and replacing $H|_L$ with its parameterization (3.3) evaluated at $X = L$, leads to (3.6). Under the regime where the consolidated ice-sheet thickness H is assumed constant, and is hereafter denoted by H_c, the equilibrium width L_c is given by $L_c = H_c U/F$ (Ou 1988; Morales Maqueda & Willmott 1999), and depends only the transport of consolidated new ice and the rate of frazil ice production. In addition to these two quantities, the equilibrium width L also depends on the offshore frazil ice velocity component.

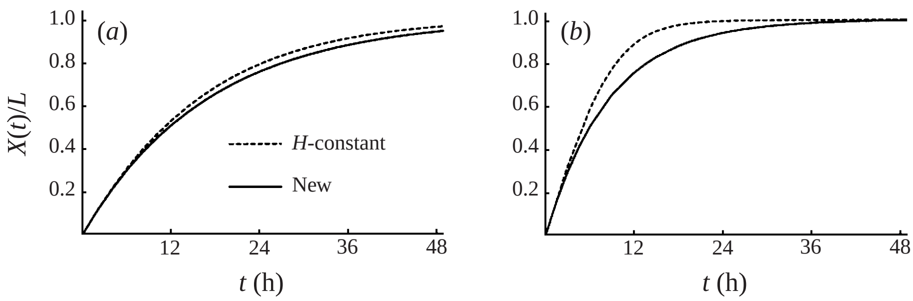

FIGURE 2. Temporal evolution of a one-dimensional polynya edge for two values of the ratio U/u: (*a*) 0.2, (*b*) 0.6.

Notice that $L > 0$, since by assumption $u > U$, and furthermore that $X \to L$ as $t \to \infty$, from (3.5). However, a finite polynya spin-up time can be defined by considering the time t^ϵ required for the polynya to open to a particular fraction of L, namely $X(t^\epsilon) \equiv X^\epsilon = (1-\epsilon)L$, where $0 < \epsilon \ll 1$. From (3.5) it is readily shown that

$$t^\epsilon = -\frac{L}{U}\ln\epsilon. \tag{3.7}$$

The quantity L/U is simply the time required for the consolidated new ice to traverse the steady-state width of the polynya, and is typically of the order of a few hours to one day at most.

It is informative to compare the spin-up time (3.7) with that obtained from the H-constant theory in which $H = H_c$. Denoting the spin-up time for the H-constant theory by t_c^ϵ, it is found by integrating (3.1), with H replaced by H_c, that

$$t_c^\epsilon = \frac{L_c}{u}(1-\epsilon) - L_c\left[\frac{1}{U} - \frac{1}{u}\right]\ln\epsilon. \tag{3.8}$$

For a valid comparison of t^ϵ and t_c^ϵ, or indeed of any of the characteristic length scales or time scales of the two problems, we must ensure that the depth of consolidated new ice at the new equilibrium polynya edge, namely $H|_L$, is equal to H_c, the consolidated new ice depth at the H-constant equilibrium polynya edge. The velocities u and U are mostly restricted to those which give the consolidated new ice depth H_c as 0.07–0.35 m, which is consistent with observations (Martin 1981). This choice of H_c also clearly leads to identical equilibrium widths L and L_c. Then, from (3.7) and (3.8),

$$t^\epsilon - t_c^\epsilon = -(L/u)[(1-\epsilon) + \ln\epsilon] > 0,$$

which shows that spin-up time associated with the collection depth parameterization (3.3) is longer than that given by the H-constant theory. Further, we see that

$$\frac{t^\epsilon - t_c^\epsilon}{t^\epsilon} = \frac{U}{u}\left[\frac{1-\epsilon}{\ln\epsilon} + 1\right] \lessapprox U/u < 1, \tag{3.9}$$

so that the relative difference between the time scales t^ϵ and t_c^ϵ depends solely on the ratio of the offshore consolidated new ice and frazil ice velocities.

The relationship between t^ϵ and t_c^ϵ is illustrated clearly in figure 2, which shows the evolution of the one-dimensional polynya edge to its steady-state width for the new and H-constant representations of the consolidated new ice collection depth H, and two values of the ratio U/u. Following Morales Maqueda & Willmott (1999), we take the frazil ice production rate as $F = 0.27\,\mathrm{m\,day^{-1}}$. For figure 2(*a*), we

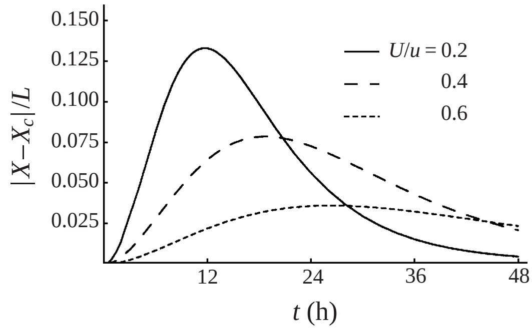

FIGURE 3. The discrepancy between the new and H-constant one-dimensional polynya edges as a function of time, for various values of the ratio U/u. In each case, the new and H-constant equilibrium widths, L and L_c, have been chosen equal through choice of H_c.

choose $u = 0.6\,\mathrm{m\,s^{-1}}$ and $U = 0.12\,\mathrm{m\,s^{-1}}$, which gives the ratio $U/u = 0.2$, and the equilibrium width $L = 7.35$ km. From (3.9), we expect the difference in the adjustment time scales to be minimal, which is indeed confirmed by the plot. In fact, using $\epsilon = 0.01$ in (3.7) and (3.8) gives $t^\epsilon \approx 78$ h and $t_c^\epsilon \approx 66$ h, respectively. In contrast, in figure 2(*b*), U is chosen to be $0.36\,\mathrm{m\,s^{-1}}$ so that $U/u = 0.6$. Now (3.9) predicts that the H-constant theory produces a polynya edge that approaches its asymptotic width considerably more quickly than that found with the new parameterization, and this is again confirmed by the plot. In this case, the time scales are $t^\epsilon \approx 39$ h and $t_c^\epsilon \approx 21$ h.

The plot in figure 3 shows to what extent the evolution of the polynya edges described by the new and H-constant theory can differ. With $u = 0.6\,\mathrm{m\,s^{-1}}$ and for small values of $U/u \approx 0.2$, the difference in the location of the polynya edges during the spin-up is minor, as predicted by (3.9). However, as U approaches u, there are times during the spin-up when the location of the polynya edges is significantly different; for example, when $U/u = 0.6$, at $t \approx 12$ h, this difference is as large as $0.13L$.

4. Sensitivity to wind speed and air temperature

To study the sensitivity of the one-dimensional polynya model with the new frazil ice collection depth law (3.3), we determine how the equilibrium width L and the spin-up time $t^{0.05}$ (the time taken for the polynya to open to $0.95L$) vary when the wind speed (U_a) and the air temperature (T_a) are independently varied. Following Pease (1987), the rate of frazil ice production, F, is determined by

$$F = \frac{-[\sigma e_a T_a^4 - Q_{lu} + \rho_a C_h C_p U_a (T_a - T_w)]}{\rho_i L_f},$$

where $\sigma = 5.67 \times 10^{-8}\,\mathrm{W\,m^{-2}\,K^{-4}}$ is the Stefan–Boltzmann constant, $e_a = 0.95$ is the emissivity of the air, $Q_{lu} = 301\,\mathrm{W\,m^{-2}}$ is the upward long-wave radiation, $\rho_a = 1.30\,\mathrm{kg\,m^{-3}}$ is the air density, $C_h = 2.0\times10^{-3}$ is the sensible heat coefficient, $C_p = 1004\,\mathrm{J\,deg^{-1}\,kg^{-1}}$ is the specific heat of air, $T_w = -1.8$°C is the water temperature, $\rho_i = 0.95\times10^3\,\mathrm{kg\,m^{-3}}$ is the ice density, and $L_f = 3.34\times10^5\,\mathrm{J\,kg^{-1}}$ is the latent heat of fusion. Following Pease (1987), the consolidated new ice velocity is $U = 0.03U_a$, and the frazil ice velocity is $u = 2U$ (Morales Maqueda & Willmott 1999). For comparison purposes, solutions are also presented for a polynya in which a constant frazil ice

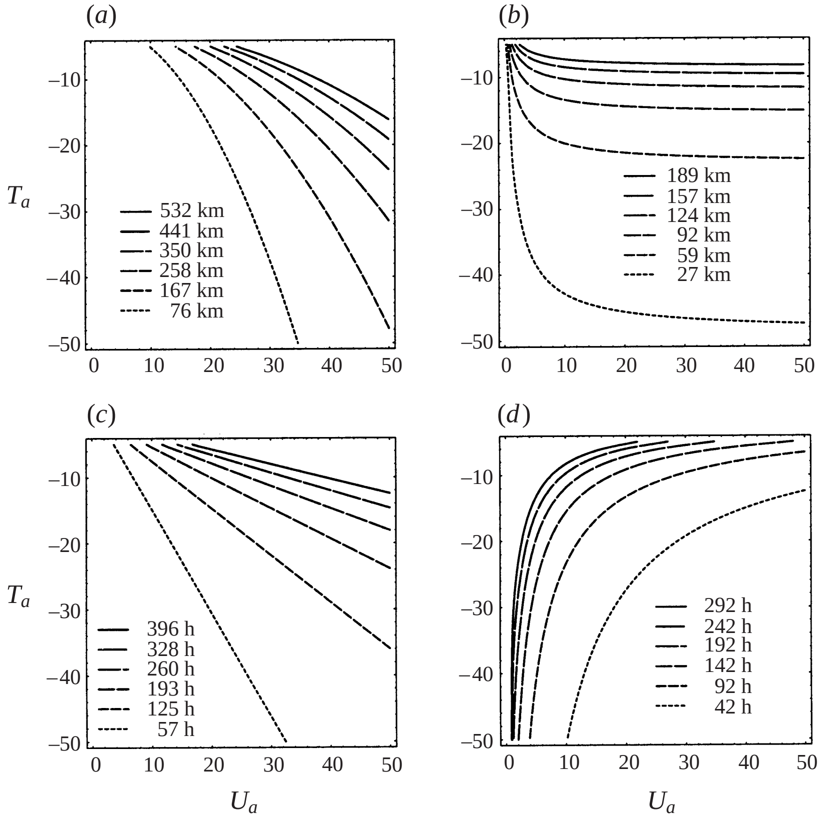

FIGURE 4. Contour plots of the new and H-constant equilibrium widths L and L_c, (*a*) and (*b*), respectively (in km), and the corresponding spin-up times $t^{0.05}$ and $t_c^{0.05}$, (*c*) and (*d*) respectively (in hours), as a function of air temperature T_a (°C) and wind speed U_a ($\mathrm{m\,s^{-1}}$). For plots (*b*) and (*d*), the constant collection thickness H_c is chosen so that $L = L_c$ at the control wind speed of $U_a = 20\,\mathrm{m\,s^{-1}}$.

collection depth, H_c, is adopted. H_c is chosen equal to 0.48 m so that for the standard wind speed of Pease (1987), $U_a = 20\,\mathrm{m\,s^{-1}}$, the frazil ice collecting at the new and H-constant equilibrium widths, $L = (cu/F)U(u - U)$ and $L_c = H_cU/F$ respectively, is of equal depths. This is equivalent to choosing the value of H_c so that the equilibrium widths are equal. We note that although the value $H_c = 0.48$ m is rather large, this choice has the advantage that it allows direct comparison with the results of Pease (1987).

Figure 4 shows that the new equilibrium width L is more sensitive to variations in wind speed than the H-constant width L_c. When $-40°\mathrm{C} \lesssim T_a \lesssim -10°\mathrm{C}$, L_c is virtually insensitive to changes in U_a, because both U and F increase linearly with increasing U_a. Increasing U tends to open the polynya, while increasing F tends to close it, and the two processes cancel. In contrast, L grows quadratically with U_a (with $u = 2U$ and $U = 0.03U_a$ we find $L = 0.000054(c/F)U_a^3$), and for $U_a \gtrsim 20\,\mathrm{m\,s^{-1}}$, $L > L_c$. For example, when $U_a = 25\,\mathrm{m\,s^{-1}}$ and $T_a = -20°\mathrm{C}$, $L \approx 140$ km while $L_c \approx 90$ km. The effect on L of varying the air temperature is comparable to its effect on L_c, since the only dependence on T_a is through the factor F^{-1} which occurs in an identical manner in the expressions for L and L_c. For lower temperatures, the frazil ice production is increased and smaller polynyas are produced, whilst warmer air temperatures cause less frazil ice to be produced and the polynya will grow larger before reaching equilibrium.

The time taken for the polynya to reach 95% of its equilibrium width is also a strong function of both wind speed and air temperature. For colder air, the ice production rate increases, resulting in smaller polynyas whose steady-state widths take shorter lengths of time to achieve. Conversely, for warmer air temperatures, the spin-up times are longer since the polynyas formed are correspondingly larger. These characteristics are shared by the H-constant spin-up time $t_c^{0.05}$. Where the two time-scales differ considerably however, is in their response to changes in wind speed, for while $t_c^{0.05}$ decreases with U_a, for $t^{0.05}$ the effect is reversed. For example, with the air temperature equal to $-20°$C and the wind speed at $20\,\mathrm{m\,s^{-1}}$, $t^{0.05} \approx 122$ h and $t_c^{0.05} \approx 81$ h. Increasing U_a by $5\,\mathrm{m\,s^{-1}}$ causes an increase in the new spin-up time to about 156 h, but a decrease in the H-constant spin-up time to 66 h. This behaviour is due to the increased dependence of L (compared with L_c) on the wind speed. In the H-constant theory, an increase in U_a leads to a linear increase in both U and u, and (3.8) shows that $t_c^{0.05}$ depends on U_a via the factor F^{-1}. On the other hand, (3.7) shows that $t^{0.05}$ grows linearly with U_a.

To summarize, both the maximum polynya width L and the spin-up time $t^{0.05}$ associated with the polynya solution using the new frazil ice collection depth law (3.3) are affected by air temperature in a similar way to their H-constant counterparts, L_c and $t_c^{0.05}$. This is because the air temperature only appears through the factor F^{-1} which occurs in the expressions for L and L_c (and thus $t^{0.05}$ and $t_c^{0.05}$) identically. The differences in the steady-state polynya widths and the spin-up times depend strongly on wind speed, because L increases quadratically with U_a, whereas L_c is almost independent of U_a when $U_a \gtrsim 10\,\mathrm{m\,s^{-1}}$. For wind speeds greater than about $20\,\mathrm{m\,s^{-1}}$, L and $t^{0.05}$ both exceed L_c and $t_c^{0.05}$, respectively. Around the coast of Antarctica, where the offshore katabatic wind speed is large, these results suggest that polynya flux models should incorporate the new frazil ice collection depth law.

5. Two-dimensional steady-state polynya adjacent to a straight semi-infinite coastal barrier

For the steady-state problem, the polynya edge is a curve along which the normal fluxes of frazil and consolidated new ice balance. Thus, writing $\boldsymbol{n}$ as the unit vector perpendicular to the polynya edge, directed away from the interior of the polynya, we demand that

$$(H\boldsymbol{U})\cdot\boldsymbol{n} = (h_C\boldsymbol{u})\cdot\boldsymbol{n}, \tag{5.1}$$

where $\boldsymbol{U} = (U, V)$ is the consolidated new ice velocity and $\boldsymbol{u} = (u, v)$ is the frazil ice velocity.

Morales Maqueda & Willmott (1999) formulate a general time-dependent polynya flux theory, and in particular they show that if $\mathscr{C}(\boldsymbol{R}, t) = $ constant denotes the polynya edge, then it satisfies

$$\nabla\mathscr{C}\cdot\left\{\frac{H\boldsymbol{U} - h_C\boldsymbol{u}}{H - h_C}\right\} + \frac{\partial\mathscr{C}}{\partial t} = 0, \tag{5.2}$$

where $\boldsymbol{R}$ is the position vector of any point on the edge. The characteristic curves of (5.2) are given by

$$\frac{\mathrm{d}\boldsymbol{R}}{\mathrm{d}t} = \frac{H\boldsymbol{U} - h_C\boldsymbol{u}}{H - h_C}. \tag{5.3}$$

In this section we will focus on steady solutions of (5.2), when H is given by (2.12). For the steady problem, let the coordinates of any point on $\mathscr{C}(\boldsymbol{R}) = \text{constant}$ be given by $(X, Y(X))$. Then $\mathscr{C}$ is given by the solution of

$$\frac{\mathrm{d}Y}{\mathrm{d}X} = \frac{HV - h_C v}{HU - h_C u}, \tag{5.4}$$

where, from (2.12), H satisfies

$$H = h_C + c|(\boldsymbol{u} - \boldsymbol{U}) \cdot \boldsymbol{n}|^2. \tag{5.5}$$

Substituting (5.5) into (5.4) yields a cubic equation for $(\mathrm{d}Y/\mathrm{d}X)$ which is given by

$$\left\{ h_C + \frac{c[(u-U)\mathrm{d}Y/\mathrm{d}X - (v-V)]^2}{[1+(\mathrm{d}Y/\mathrm{d}X)^2]} \right\} \left[U\frac{\mathrm{d}Y}{\mathrm{d}X} - V \right] = h_C \left[u\frac{\mathrm{d}Y}{\mathrm{d}X} - v \right]. \tag{5.6}$$

Now consider a semi-infinite straight coastline coinciding with the negative y-axis, and assume that the polynya edge lies in the quadrant $x > 0$, $y < 0$, and passes through the origin located at the end of the coastal wall. When $\boldsymbol{u}$ and $\boldsymbol{U}$ are both constant, the steady-state frazil ice mass conservation equation is

$$u\frac{\partial h}{\partial x} + v\frac{\partial h}{\partial y} = F. \tag{5.7}$$

The solution of (5.7) satisfying $h(0, y) = 0$, $y < 0$, is given by $h = Fx/u$, provided that F is constant. Therefore, $h_C = FX/u$, which upon substitution into (5.6) and factorising, yields three possible differential equations for the polynya edge, namely

$$\frac{\mathrm{d}Y_1}{\mathrm{d}X} = \frac{v - V}{u - U},$$

$$\frac{\mathrm{d}Y_2}{\mathrm{d}X} = \frac{-A - [B^2 - 4X(X - C)]^{1/2}}{2(X - L)},$$

$$\frac{\mathrm{d}Y_3}{\mathrm{d}X} = \frac{-A + [B^2 - 4X(X - C)]^{1/2}}{2(X - L)},$$

where for brevity we have introduced the notation

$$A = (cu/F)[U(v - V) + V(u - U)],$$
$$B = (cu/F)[U(v - V) - V(u - U)],$$
$$C = (cu/F)[U(u - U) + V(v - V)],$$

and $L = (cu/F)U(u - U)$ denotes the equilibrium width.

The straight line solution $Y_1(X) = [(v - V)/(u - U)]X$ is oriented parallel to the relative velocity $\boldsymbol{u} - \boldsymbol{U}$. For this solution, the normal is such that $(\boldsymbol{u} - \boldsymbol{U}) \cdot \boldsymbol{n} = 0$, in which case $H = h_C$, and the differential equation for Y_1 is recovered immediately from (5.4). From a physical point of view, this solution can be discarded, for the following reason. Let $\tan\alpha = v/u$ and $\tan\theta = V/U$, where α and θ denote the angles (measured positive in a counterclockwise sense) made by $\boldsymbol{u}$ and $\boldsymbol{U}$ with the positive x-axis, respectively. For wind speeds of $3\,\mathrm{m\,s^{-1}}$, or more, frazil ice is observed to drift along wind rows associated with Langmuir circulations Martin & Kauffman (1981). The wind rows are oriented at an angle of 13°, or less, to the right of the wind stress (in the Northern Hemisphere). In this study we will assume that $\boldsymbol{u}$ is parallel to the surface wind stress. However, the consolidated new ice drift is influenced by the structure of the wind-driven surface Ekman layer, and hence $\boldsymbol{U}$ is oriented at an angle of 28° to the right of the wind stress (in the Northern Hemisphere). More generally, we assume only that $\boldsymbol{U}$ is oriented to the right of $\boldsymbol{u}$, so that $\alpha > \theta$. Then since

$$\frac{v}{u} - \frac{v-V}{u-U} = \frac{|\boldsymbol{u}||\boldsymbol{U}|\sin(\alpha-\theta)}{u(u-U)} > 0,$$

we see that $Y_1(X)$ is oriented to the left of $\boldsymbol{u}$. The frazil ice trajectory passing through the origin must lie in the consolidated new ice region and therefore starting from a polynya of zero width, we can never spin-up to the solution $Y_1(X)$.

We can also reject the solution $Y_2(X)$ on similar grounds to $Y_1(X)$. Notice that at the origin $\mathrm{d}Y_2/\mathrm{d}X = (v-V)/(u-U)$. In fact $\mathrm{d}Y_2/\mathrm{d}X \geqslant (v-V)/(u-U)$ for $x \in [0, L]$, and as $x \to L$, $\mathrm{d}Y_2/\mathrm{d}X \to \infty$. The solution $Y_2(X)$ lies inside the quadrant $X \geqslant 0$, $Y \geqslant 0$ and it smoothly attains its asymptotic width $X = L$. However, because the frazil ice trajectory passing through the origin lies wholly within the consolidated new ice region we reject this solution for the same reason as rejecting $Y_1(X)$.

Now consider the differential equation for $Y_3(X)$, where for notational convenience, we henceforth drop the subscript 3:

$$\frac{\mathrm{d}Y}{\mathrm{d}X} = \frac{-A + [B^2 - 4X(X-C)]^{1/2}}{2(X-L)}, \quad Y(0) = 0. \tag{5.8}$$

It is straightforward to integrate (5.8), subject to the condition $Y(0) = 0$, to obtain

$$\begin{aligned} 2Y(X) = {} & [B^2 - 4X(X-C)]^{1/2} - B + (2L - C)\arctan(-C/B) \\ & -(2L-C)\arctan\left[\frac{2X-C}{[B^2-4X(X-C)]^{1/2}}\right] + (A - |A|)\ln\left(\frac{L}{L-X}\right) \\ & -|A|\ln\left[\frac{B^2 - 4LX + 2C(X+L) + |A|[B^2-4X(X-C)]^{1/2}}{B^2 + 2CL + |A|B}\right], \end{aligned} \tag{5.9}$$

where we have used the fact that $B = (cu/F)|\boldsymbol{U}||\boldsymbol{u}|\sin(\alpha-\theta) > 0$, since $(\alpha - \theta) > 0$.

The solution (5.9) clearly exhibits three distinct types of behaviour, depending on the sign of the constant A. Suppose, first, that $A < 0$. Then as $X \to L^-$ (i.e. approaches the equilibrium width L from below), the denominator of the right-hand side of (5.8) approaches zero from below, while the numerator tends to $-A + [B^2 - 4L(L-C)]^{1/2} = -A + [A^2]^{1/2} = -2A > 0$. Thus $\mathrm{d}Y/\mathrm{d}X \to -\infty$ as $X \to L^-$, and the polynya reaches its equilibrium width asymptotically, and from (5.9) it achieves this width as $Y \to -\infty$. However, now suppose that $A > 0$. Now as $X \to L^-$, the numerator of the right-hand side of (5.8) tends to $-A + [B^2 - 4L(L-C)]^{1/2} = -A + [A^2]^{1/2} = 0$. Application of l'Hôpital's rule then shows that $\mathrm{d}Y/\mathrm{d}X = -(2L-C)/A > -\infty$ as $X \to L^-$. In this case, (5.9) shows that the polynya edge reaches its steady-state width at $Y = -Y_L$, where

$$Y_L = L\left|\tan\theta + (\gamma - \pi/2)(1 - \tan\theta\tan\gamma) - \frac{\sin(\theta+\gamma)}{\cos\theta\cos\gamma}\ln\left[\frac{\sin(\theta+\gamma)}{\cos\theta}\right]\right|, \tag{5.10}$$

and γ denotes the angle the relative velocity $\boldsymbol{u} - \boldsymbol{U}$ makes with the positive x-axis. The polynya edge thus exhibits a corner at $(L, -Y_L)$; for $Y < -Y_L$, the equation of the edge is the straight line $X = L$. Recalling that $\tan\theta = V/U$, we see that $A = (cu/F)|\boldsymbol{U}||\boldsymbol{u} - \boldsymbol{U}|\sin(\theta+\gamma)$, and the requirement for the existence of a corner is

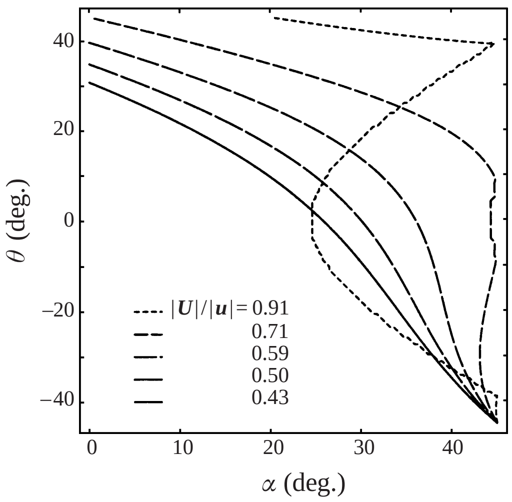

FIGURE 5. Plot of the curves $(\theta+\gamma)=0$ for various values of the ratio $|\boldsymbol{U}|/|\boldsymbol{u}|$. Points to the right of the curves correspond to $(\theta+\gamma)>0$.

simply $\theta+\gamma>0$. We can re-write this inequality in terms of α and θ by noting that

$$\gamma=\theta+\arcsin\left[\frac{|\boldsymbol{u}|}{|\boldsymbol{u}-\boldsymbol{U}|}\sin(\alpha-\theta)\right],$$

in which case a corner will occur on the edge when

$$2\theta+\arcsin\left[\frac{|\boldsymbol{u}|}{|\boldsymbol{u}-\boldsymbol{U}|}\sin(\alpha-\theta)\right]>0.$$

Figure 5 shows the line $\theta+\gamma=0$ in the (α,θ)-plane for a variety of values of the ratio $|\boldsymbol{U}|/|\boldsymbol{u}|$; points to the right of these lines correspond to $\theta+\gamma$ positive, giving a corner. The range of (α,θ) for which a corner is produced is greatest when either $|\boldsymbol{u}|$ and $|\boldsymbol{U}|$ are comparable in magnitude, or when they differ by a factor of 2 or more. Intermediate values of $|\boldsymbol{U}|/|\boldsymbol{u}|$ (≈ 0.66) minimize the likelihood of a corner.

Finally, consider the case when $A=0$, which is equivalent to $\theta+\gamma=0$. As $X\to L$, (5.8) shows that $\mathrm{d}Y/\mathrm{d}X\to-\infty$, and once again the polynya edge smoothly approaches $X=L$. However, the polynya edge solution corresponding to taking the limit $A\to 0$ in (5.9) is finite at $X=L$, so that the polynya edge in fact reaches its equilibrium width at $Y=-Y_L^0$, where

$$Y_L^0=L|\tan\theta-(\theta+\pi/2)\sec^2\theta| \tag{5.11}$$

is obtained by considering the limit $(\theta+\gamma)\to 0$ in (5.10).

Why does the sign of $\theta+\gamma$ determine whether, or not, $\mathscr{C}$ has a corner? To answer this, we consider the depth of frazil ice arriving at any point P on $\mathscr{C}$. Solving (5.6) for h_C, we obtain

$$h_C=\frac{c[(u-U)\mathrm{d}Y/\mathrm{d}X-(v-V)][U\mathrm{d}Y/\mathrm{d}X-V]}{[1+(\mathrm{d}Y/\mathrm{d}X)^2]},$$

and if ϕ denotes the angle between the tangent to $\mathscr{C}$ at P and the positive x-axis, we find that

$$h_C=\tfrac{1}{2}c|\boldsymbol{U}||(\boldsymbol{u}-\boldsymbol{U})|[\cos(\theta-\gamma)-\cos(\theta+\gamma-2\phi)]. \tag{5.12}$$

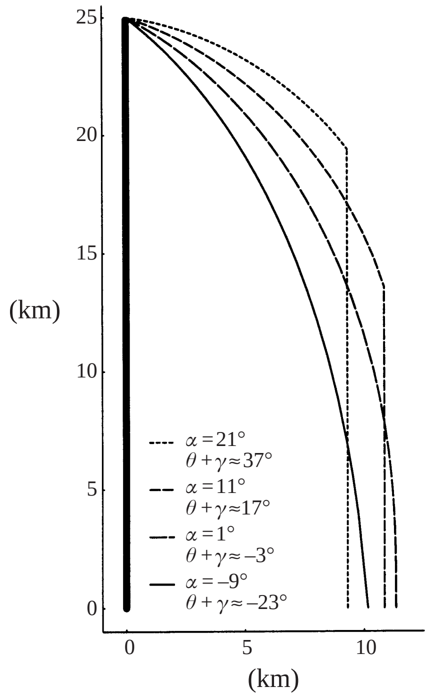

FIGURE 6. The effect of rotating the directions of frazil ice drift and consolidated new ice drift on the new polynya edge solutions adjacent to a semi-infinite straight coastline (vertical bold line). For all cases, $F = 0.27\,\mathrm{m\,day^{-1}}$, $|\boldsymbol{u}| = 0.6\,\mathrm{m\,s^{-1}}$, $|\boldsymbol{U}| = 0.3\,\mathrm{m\,s^{-1}}$, and the angle between $\boldsymbol{u}$ and $\boldsymbol{U}$ is fixed at 28°.

For a given polynya edge, α and θ and thus γ are fixed, and when $\phi = \phi^{\max} = (\theta + \gamma - \pi)/2$, h_C attains a maximum value

$$h_C^{\max} = \tfrac{1}{2}c|\boldsymbol{U}||(\boldsymbol{u} - \boldsymbol{U})|[1 + \cos(\theta - \gamma)]. \tag{5.13}$$

Notice that (5.13) is only achieved at the equilibrium width when $\theta + \gamma = 0$, when $\phi^{\max} = -\pi/2$. More generally,

$$\begin{aligned} h_C^{\max} - h_C(L) &= c|\boldsymbol{U}||(\boldsymbol{u} - \boldsymbol{U})|\{\tfrac{1}{2}[1 + \cos(\theta - \gamma)] - \cos\theta\cos\gamma\} \\ &= c|\boldsymbol{U}||(\boldsymbol{u} - \boldsymbol{U})|\sin^2[(\theta + \gamma)/2] \geqslant 0. \end{aligned}$$

If $\theta + \gamma < 0$, $h_C^{\max}$ is reached when $\phi^{\max} < -\pi/2$, which is impossible since ϕ is clearly bounded below by $-\pi/2$. Alternatively, if $\theta + \gamma > 0$, $h_C^{\max} > h_C(L)$, and the maximum frazil ice depth occurs at a point further offshore, where $\phi^{\max} > -\pi/2$. At this point the solution breaks down, since its continuation would require frazil ice of depth $h_C > h_C^{\max}$. The presence of the corner on $\mathscr{C}$ when $\theta + \gamma > 0$ leads to a solution in which $h_C < h_C^{\max}$, for all points on $\mathscr{C}$.

Figure 6 shows plots of (5.9) for various values of α and θ, which exhibit the types of behaviour discussed above. In figure 6, $F = 0.27\,\mathrm{m\,day^{-1}}$ (following Morales Maqueda & Willmott 1999), $|\boldsymbol{U}| = 0.3\,\mathrm{m\,s^{-1}}$, $|\boldsymbol{u}| = 2|\boldsymbol{U}|$, $\alpha - \theta = 28°$ for all the solutions, and the four edges correspond to $\alpha = -9°, 1°, 11°, 21°$, which give $\theta + \gamma \approx -23°, -3°, 17°, 37°$ respectively. The polynya edges shown in figure 6 exhibit a corner when $\theta + \gamma > 0$, but when $\theta + \gamma \leqslant 0$, the edge reaches the asymptotic width $X = L$ smoothly.

Also shown (figure 7) is a comparison between the polynya edge solutions for the new and H-constant formulations of the frazil ice collection depth H. In figure 7,

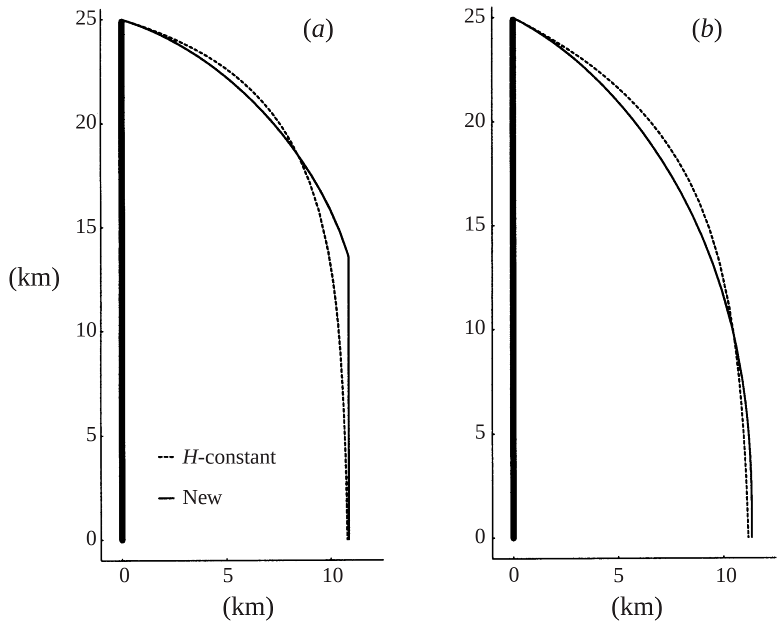

FIGURE 7. New and H-constant polynya edge solutions adjacent to a semi-infinite straight coastline (vertical bold line). In (*a*), $\alpha = 11°$ and $\theta = -17°$, while in (*b*), $\alpha = 1°$ and $\theta = -27°$. F, $|\boldsymbol{u}|$, and $|\boldsymbol{U}|$ are the same as in the previous figure.

$|\boldsymbol{U}|$, $|\boldsymbol{u}|$, and F are as in figure 6. In figure 7(*a*), the orientations of the frazil ice and consolidated new ice velocities are given by $\alpha = 11°$ and $\theta = -17°$, so that $\theta + \gamma \approx 27° > 0$. Hence a corner is produced on the new edge. Notice that the area of the new polynya in the finite region $\Lambda = \{(x, y) : 0 < x < L,\ -\infty < -y^* < y < 0\}$, where $-y^* \leqslant -Y_L$, is larger than the area of the H-constant polynya. In contrast, the edge plotted in figure 7(*b*) is generated for $\alpha = 1°$ and $\theta = -27°$ so that $\theta + \gamma \approx -3° < 0$, and no corner is exhibited. The difference in this case between the H-constant and new solutions is minimal, although the area contained by the H-constant edge appears greater. Indeed, if a corner is exhibited by the polynya edge, the area contained by it in the finite region Λ generally exceeds the area of the corresponding H-constant polynya, while the reverse happens if no corner is produced. Figure 8 shows this idea clearly for the particular parameter values $|\boldsymbol{U}| = 0.2\,\mathrm{m\,s^{-1}}$, $|\boldsymbol{u}| = 0.6\,\mathrm{m\,s^{-1}}$, and $F = 0.27\,\mathrm{m\,day^{-1}}$, and a range of values of θ, with $\alpha - \theta = 28°$. In figure 8, the unbroken line represents the area contained by the new polynya edge, while the dashed line represents the area contained by the H-constant polynya edge. The polynya area exceeds the H-constant polynya area for $\theta \gtrsim -16°$ whilst a corner is exhibited in the new polynya edge for $\theta \gtrsim -20°$.

Morales Maqueda & Willmott (1999) show the importance of the alongshore adjustment length-scale associated with a two-dimensional polynya in controlling the relationship between variations in the orientation of the coastline and the shape of the polynya edge. Let us now determine the alongshore adjustment length scale, L^a, associated with the solution (5.9). To this end, we introduce a small coastline perturbation which produces a corresponding perturbation in the polynya edge. Suppose that the coastal boundary is given by the straight line $x = 0$ except in the interval $I = \{y : y_1 < y < y_2\}$, where the coastline is given by $x = f(y)$, with $|f(y)| \ll L$, and $f(y_1) = f(y_2) = 0$. In order to ensure that frazil ice leaving the

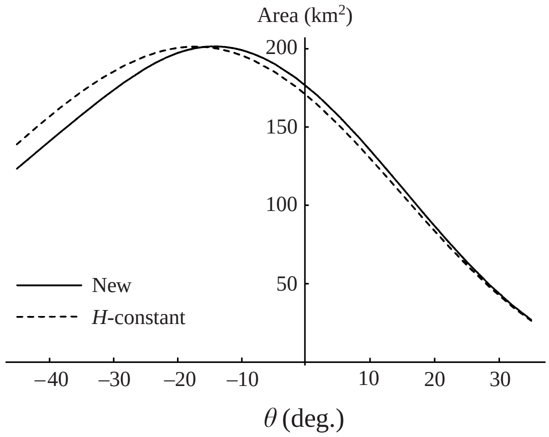

FIGURE 8. New and H-constant polynya areas (in km^2) contained in the finite regions bounded by the coastline, the polynya edge, and a line perpendicular to the coast 25 km (in the negative y-direction) from the polynya coastal intersection point, for varying θ. $|\boldsymbol{u}| = 0.6\,\mathrm{m\,s^{-1}}$, $|\boldsymbol{U}| = 0.3\,\mathrm{m\,s^{-1}}$, F is the same as in previous plots, and the frazil ice drifts in a direction $\alpha = 28° + \theta$. A corner is exhibited in the polynya edge when $\theta \gtrsim -20.3°$.

coastline cannot subsequently intercept it again, we demand that $|\mathrm{d}f/\mathrm{d}y| < |\tan\alpha|$. Now, the coordinates of any point on the equilibrium polynya edge can be written as $P = (L + X', Y)$, where X' is the perturbation induced by the coastline irregularities, and $|X'| \ll L$. Then the frazil ice trajectory intercepting P is given by $y = (v/u)[x - (L + X')] + Y$, and leaves the coastal point Q whose x-coordinate is, to first order in the perturbation, $x'_Q = f(Y - (v/u)L)$. Thus, the offshore distance travelled by the frazil ice on the trajectory QP is $L + X' - f(Y - (v/u)L)$, and the thickness of frazil ice arriving at P is given by $h_C = (F/u)L + (F/u)\{X' - f(Y - (v/u)L)\}$. From (5.4) we can then show that X' satisfies the differential equation

$$\frac{L\sin(\theta+\gamma)}{\cos\theta\cos\gamma}\frac{\mathrm{d}X'}{\mathrm{d}Y} = -[X' - f(Y - (v/u)L)], \tag{5.14}$$

again to first order in the perturbation. Provided $\theta + \gamma \neq 0$, (5.14) can be written as

$$\frac{\mathrm{d}X'}{\mathrm{d}Y} = [X' - f(Y - (v/u)L)]/L^a, \tag{5.15}$$

where

$$L^a = \frac{-L\sin(\theta+\gamma)}{\cos\theta\cos\gamma} \tag{5.16}$$

is the alongshore adjustment length scale that controls how sensitive the steady-state polynya edge is to small irregularities in the coastline. Rewriting (5.16) as

$$L^a = -L[\tan\theta + \tan\gamma] = -L\left[\frac{V}{U} + \frac{v-V}{u-U}\right]$$

leads to a geometrical visualization of this quantity. A consolidated ice trajectory leaving the coast from $y = y^*$ will, upon reaching the equilibrium width L, have travelled an alongshore distance LV/U from $y = y^*$. Similarly, a trajectory leaving the coast from $y = y^*$ parallel to the relative velocity $\boldsymbol{u} - \boldsymbol{U}$, will have travelled an alongshore distance $L(v - V)/(u - U)$ from $y = y^*$. The magnitude of the alongshore adjustment length scale $|L^a|$ is then simply the sum of these two distances.

A physical interpretation of the quantity L^a is, however, afforded by the following analysis. The normal vector to the unperturbed equilibrium edge $X = L$ is simply $\boldsymbol{n} = (1, 0)$, while frazil ice reaching this steady-state edge is of depth $h_C(L) \equiv h_C^{(L)} = c|\boldsymbol{U}||\boldsymbol{u} - \boldsymbol{U}|\cos\theta\cos\gamma$. Perturbing the coastal profile, as we have seen above, causes a corresponding perturbation in the polynya edge. This can be represented by replacing $\boldsymbol{n}$ with $\boldsymbol{n}' = (\cos\delta, \sin\delta)$, where $0 < |\delta| \ll 1$ is measured positive in a counterclockwise sense from the positive x-axis. Denoting the depth of frazil ice reaching the perturbed polynya edge by $h_C^{(L)'}$, it is then easy to show that

$$h_C^{(L)'} = h_C^{(L)} - \delta \frac{F}{u} L^a. \tag{5.17}$$

Letting $\delta \to 0$ in (5.17) leads to

$$\frac{\mathrm{d}\rho}{\mathrm{d}\sigma} = -L^a,$$

where σ is the angle between $\boldsymbol{n}$ and the positive x-axis, and $\rho = uh_C^{(L)}/F$ is the distance travelled by frazil ice from the coast to the polynya edge.

These ideas prove important in determining X', for we must consider the cases $\theta+\gamma < 0$ and $\theta+\gamma > 0$ separately. If $\theta+\gamma < 0$, then from (5.16), $L^a > 0$. In this case, we must integrate (5.15) in the negative y-direction from $Y = Y_2$, since for $Y \geqslant Y_2$, the polynya edge is unaffected by the coastal perturbation, and satisfies $X = L$. Why is this so? Suppose that this is not the case, and that the polynya edge differs from $X = L$ for $Y \geqslant Y_2$. At some distance away in the positive y-direction, the edge must approach the steady-state width $X = L$, and will do so from either $X < L$ or $X > L$. If it approaches $X = L$ from below ($X < L$), then the angle $\boldsymbol{n}$ makes with the positive x-axis here is negative, and (5.17) implies that the depth of frazil ice reaching the polynya edge here is greater than that reaching the width $X = L$. This is clearly impossible since the frazil ice depth $h(x) = Fx/u$ is a monotonically increasing function of offshore distance, x. A similar contradiction arises if the polynya edge asymptotes towards $X = L$ from above ($X > L$). We deduce that in the case where $L^a > 0$, the polynya edge is given by $X = L$ for $Y \geqslant Y_2$, and (5.15) is then integrated with the boundary condition $X'(Y_2) = 0$ to give

$$X' = \exp\left[-(Y_2 - Y)/L^a\right] \int_Y^{Y_2} \frac{1}{L^a} f(Z - (v/u)L) \exp\left[(Y_2 - Z)/L^a\right] \mathrm{d}Z.$$

The quantity L^a influences X' in two ways. The factor $1/L^a$ in the integrand modulates the amplitude of X', whilst the presence of the term $\exp[-(Y_2 - Y)/L^a]$ provides an e-folding length scale for the decay of X' in the negative y-direction.

In contrast, if $\theta+\gamma > 0$, then from (5.16), $L^a < 0$. For reasons analogous to those described above, we now integrate (5.15) in the positive y-direction from $Y = Y_1$ where $X'(Y_1) = 0$, since $X = L$ for $Y \leqslant Y_1$. We now find that

$$X' = -\exp\left[(Y - Y_1)/L^a\right] \int_{Y_1}^{Y} \frac{1}{L^a} f(Z - (v/u)L) \exp\left[-(Z - Y_1)/L^a\right] \mathrm{d}Z.$$

Again in this expression, the factor $1/L^a$ in the integrand modulates the amplitude of X', but now the term $\exp[(Y - Y_1)/L^a]$ provides an e-folding length scale for the decay of X' in the *positive* y-direction.

When $\theta+\gamma = 0$, the differential equation (5.14) for the polynya edge perturbation X' reduces to an algebraic equation, with solution $X' = f(Y - (v/u)L)$. In this special case, the alongshore adjustment length-scale L^a is zero (which can also be seen by taking the appropriate limit of (5.16)), and the polynya edge reproduces the coastal perturbation precisely.

The change of character in the perturbed steady-state edge dependent upon the sign of $(\theta + \gamma)$ presents a marked departure from that of the H-constant perturbed edge, which decays exponentially in the negative y-direction regardless (Morales Maqueda & Willmott 1999). The contrasting behaviour described above is a consequence of the new frazil ice collection depth law, and in particular the increased dependence of H upon the gradient of the polynya edge. However, in both cases, coastal irregularities with characteristic alongshore length scales smaller than $|L^a|$ will have almost no effect on the steady-state polynya edge.

6. Steady-state polynya adjacent to a finite-length straight coastal barrier

We now consider the case where the coast is a line-segment of finite length D located on the y-axis, with end points $(0, 0)$ and $(0, D)$, with the polynya lying in the region $x > 0$. This coastal configuration can be thought of as an idealized island. In the region bounded by the straight lines $M_1 = \{(x, y)\colon Vx - Uy = 0,\ x < 0\}$, $M_2 = \{(x, y)\colon Vx - U(y - D) = 0,\ x < 0\}$ and $x = 0$, we assume that the ice is motionless; in practice, ice in this region is often of first-year type. The polynya lies within the region bounded by $N_1 = \{(x, y)\colon Vx - Uy = 0,\ x > 0\}$, $N_2 = \{(x, y)\colon Vx - U(y - D) = 0,\ x > 0\}$ and $x = 0$. Clearly, the polynya edge ($\mathscr{C}$) either passes through $(0, D)$ and does not intersect N_2 again, or $\mathscr{C}$ includes some portion of N_2. The latter case can be rejected because for any point on N_2 satisfying the flux balance $(H\boldsymbol{U}) \cdot \boldsymbol{n} = (h_C \boldsymbol{u}) \cdot \boldsymbol{n}$, we see that $h_C \boldsymbol{u} \cdot \boldsymbol{n} = 0$, which in turn implies that $h_C = 0$, because we assume that $\boldsymbol{u}$ and $\boldsymbol{U}$ are not parallel (in fact, we assume that $\boldsymbol{u}$ is oriented to the left of $\boldsymbol{U}$). Therefore the only point on N_2 that also lies on $\mathscr{C}$ is the coastal point $(0, D)$.

The polynya is divided into two distinct regions separated by the frazil trajectory emanating from the origin, namely $\Gamma = \{(x, y)\colon vx - uy = 0,\ x > 0\}$. Let A_1 denote the area of the polynya lying in region 1 defined by $\{(x, y)\colon vx - uy < 0\}$. Similarly, let A_2 denote the area of the polynya lying in region 2 defined by $\{(x, y)\colon vx - uy > 0\}$. Points on the polynya edge in region 1 receive frazil ice from the island coastline, and therefore in this region the equation of $\mathscr{C}$ is given by (5.9), with the appropriate translation of the y-coordinate to accommodate the boundary condition $Y(D) = 0$. In region 2, however, the frazil trajectories intercepting $\mathscr{C}$ emanate from the ice pack boundary N_1, since the angle between the direction of travel of the frazil and consolidated new ice is positive. The point of intersection $P = (X^{\text{int}}, Y^{\text{int}})$ of $\mathscr{C}$ with Γ is easily found analytically, provided the island is sufficiently long, and the frazil ice and consolidated new ice velocities are such that $\mathscr{C}$ has attained its asymptotic width. To be precise, if there is a corner on $\mathscr{C}$ at $(L, D - Y_L)$ (for which we require $\theta + \gamma > 0$), then $(X^{\text{int}}, Y^{\text{int}}) = (L, (v/u)L)$, provided $(v/u)L < D - Y_L$. If $(v/u)L \geqslant D - Y_L$, then Γ strikes $\mathscr{C}$ before it has reached the width L, and the coordinates of P satisfy a transcendental equation. In a similar manner, we see that if the corresponding semi-infinite coastline polynya ice edge does not exhibit a corner, then $X \to L$ as $Y \to -\infty$, and once again the coordinates of P satisfy a transcendental equation. However, for long islands ($D \gg |L^a|$) the coordinates of P can be approximated by $(L, (v/u)L)$.

The portion of $\mathscr{C}$ lying in region 2 can be determined by introducing the rotated coordinates

$$x_r = -x \sin\theta + y \cos\theta, \qquad y_r = -x \sin\theta - y \cos\theta,$$

so that the negative y_r-axis then coincides with the line N_1. In this new rotated reference frame, the frazil ice velocity components are given by $u_r = |\boldsymbol{u}| \sin(\alpha - \theta)$ and $v_r = -|\boldsymbol{u}| \cos(\alpha - \theta)$, while the consolidated new ice velocity components are $U_r = 0$ and $V_r = -|\boldsymbol{U}|$. With respect to the rotated coordinates, let $\mathscr{C}$ be given by $Y_r = Y_r(X_r)$ where Y_r satisfies the appropriately modified differential equation

$$\frac{\mathrm{d}Y_r}{\mathrm{d}X_r} = \frac{-A_r + [A_r^2 - 4X_r(X_r - C_r)]^{1/2}}{2X_r}. \tag{6.1}$$

In (6.1), A_r and C_r are constants which satisfy $A_r = (cu_r/F)u_r V_r$ and $C_r = (cu_r/F)V_r(v_r - V_r)$. Notice that $A_r < 0$, so that the polynya edge smoothly reaches the equilibrium width $X_r = (cu_r/F)U_r(u_r - U_r) = 0$, that is, the ice pack boundary N_1. The differential equation (6.1) is solved subject to the boundary condition $Y(X_r^{\mathrm{int}}) = Y_r^{\mathrm{int}}$ where $X_r^{\mathrm{int}} = -X^{\mathrm{int}} \sin\theta + Y^{\mathrm{int}} \cos\theta$ and $Y_r^{\mathrm{int}} = -(X^{\mathrm{int}} \cos\theta + Y^{\mathrm{int}} \sin\theta)$ are the coordinates of the point of intersection of $\mathscr{C}$ and Γ with respect to the rotated coordinate frame. We find that in region 2, $\mathscr{C}$ is given by

$$\begin{aligned} 2[Y_r(X_r) - Y_r^{\mathrm{int}}] &= [A_r^2 - 4X_r(X_r - C_r)]^{1/2} - [A_r^2 - 4X_r^{\mathrm{int}}(X_r^{\mathrm{int}} - C_r)]^{1/2} \\ &+ C_r \left\{ \arctan\left[\frac{2X_r - C_r}{[A_r^2 - 4X_r(X_r - C_r)]^{1/2}}\right] - \arctan\left[\frac{2X_r^{\mathrm{int}} - C_r}{[A_r^2 - 4X_r^{\mathrm{int}}(X_r^{\mathrm{int}} - C_r)]^{1/2}}\right]\right\} \\ &+ A_r \ln\left\{\left(\frac{X_r^{\mathrm{int}}}{X_r}\right)^2 \left[\frac{A_r^2 + 2C_r X_r - A_r[A_r^2 - 4X_r(X_r - C_r)]^{1/2}}{A_r^2 + 2C_r X_r^{\mathrm{int}} - A_r[A_r^2 - 4X_r^{\mathrm{int}}(X_r^{\mathrm{int}} - C_r)]^{1/2}}\right]\right\}. \end{aligned} \tag{6.2}$$

Figure 9 shows two particular steady-state polynya edges produced by the idealized island geometry. The island length is $D = 25\,\mathrm{km}$, and $\boldsymbol{u}$, $\boldsymbol{U}$ and F are as in figure 7. Notice that the transition of the polynya edge from region 1 to 2 is not smooth, as the gradient of the edge has a discontinuity at $(X, Y) = (X^{\mathrm{int}}, Y^{\mathrm{int}})$. This is a consequence of the increased coupling of the frazil ice collection depth H with the gradient of the polynya edge solution, and is in contrast with the H-constant solution, in which $\mathscr{C}$ is smooth throughout its extent.

The total area, $A_T = A_1 + A_2$, of the steady-state polynya can be determined by integration of the equation of conservation of frazil ice mass over the entire polynya, which gives

$$\iint_{A_T} \nabla \cdot (h_C \boldsymbol{u})\, \mathrm{d}S = \iint_{A_T} F\, \mathrm{d}S.$$

With the aid of the divergence theorem, when the frazil ice production rate F is spatially constant, this can be simplified to

$$A_T = \frac{1}{F} \int_{\mathscr{C}} h_C \boldsymbol{u} \cdot \boldsymbol{n}\, \mathrm{d}s, \tag{6.3}$$

where s is arc length measured along $\mathscr{C}$. The ice flux balance $(H\boldsymbol{U}) \cdot \boldsymbol{n} = (h_C \boldsymbol{u}) \cdot \boldsymbol{n}$ which holds on the polynya edge allows (6.3) to be immediately re-written as

$$A_T = \frac{1}{F} \int_{\mathscr{C}} H \boldsymbol{U} \cdot \boldsymbol{n}\, \mathrm{d}s. \tag{6.4}$$

For the H-constant case of constant frazil ice collection depth, $H \equiv H_c$, the area, $A_T^{(c)}$, of a polynya lying adjacent to a straight coastal barrier of finite length D is, from (6.4),

$$A_T^{(c)} = DH_c U/F, \tag{6.5}$$

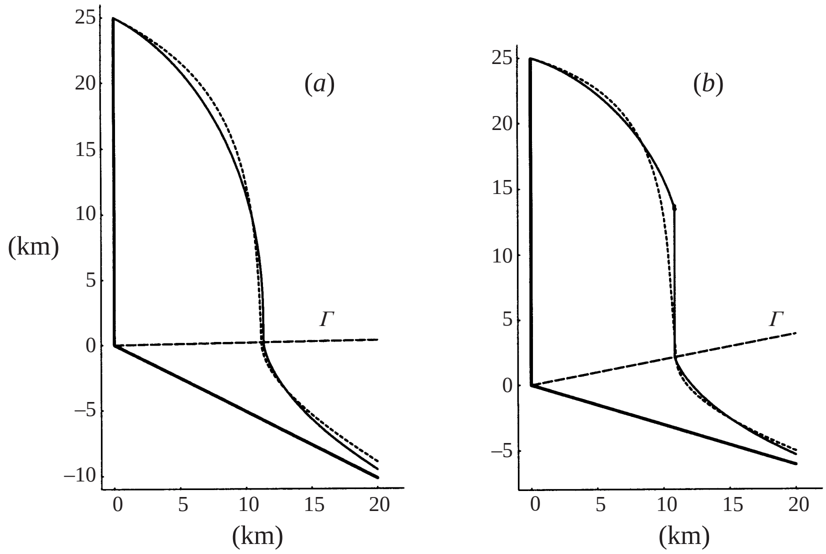

FIGURE 9. New and H-constant polynya edge solutions adjacent to a finite-length straight coastline. For (*a*), the directions of frazil ice and consolidated new ice drift are $\alpha = 1°$ and $\theta = -27°$ respectively, while for (*b*), $\alpha = 11°$ and $\theta = -17°$. In both plots, Γ denotes the critical frazil ice trajectory leaving the origin, the solid line depicts the new polynya edge, and the dashed line depicts the H-constant polynya edge. Lastly, the vertical bold line represents the coastline of the idealized island, and the angled bold line represents the border of the consolidated new ice pack.

as shown in Morales Maqueda & Willmott (1999). Unfortunately, an equally compact expression for the area does not exist when H is given by (5.5); in this case, an exact expression for A_T is best determined through direct evaluation of (6.3), but the resulting expression is complicated and not amenable to analysis and comparison with (6.5). However, upper and lower bounds on A_T can be determined by deriving upper and lower bounds for the frazil ice collection depth H.

From (5.5) and (5.12) we see that

$$H = c|\boldsymbol{U}||(\boldsymbol{u}-\boldsymbol{U})|\sin(\theta-\phi)\sin(\gamma-\phi) + \frac{c[(u-U)\mathrm{d}Y/\mathrm{d}X-(v-V)]^2}{1+(\mathrm{d}Y/\mathrm{d}X)^2},$$

where ϕ is again the angle between the tangent to the polynya edge and the positive x-axis, measured in a counterclockwise sense. Simplifying this expression leads to

$$H = \tfrac{1}{2}c|\boldsymbol{u}||(\boldsymbol{u}-\boldsymbol{U})|[\cos(\alpha-\gamma)-\cos(\alpha+\gamma-2\phi)],$$

so that H is maximized when $\alpha+\gamma-2\phi=\pi$; at this point $H = H^{\max}$, where

$$H^{\max} = \tfrac{1}{2}c|\boldsymbol{u}||(\boldsymbol{u}-\boldsymbol{U})|[1+\cos(\alpha-\gamma)]. \tag{6.6}$$

The minimum value, $H^{\min}$, occurs at either the point of intersection of the polynya edge with the coast, where $H = H^{\mathrm{coast}}$, or at the point at which the equilibrium width L is reached, where $H = H|_L$. As $\mathrm{d}Y/\mathrm{d}X = V/U$ and $h_C = 0$ at the coast, $H^{\mathrm{coast}} = c|\boldsymbol{u}|^2\sin^2(\alpha-\theta)$, whilst choosing the constant collection depth thickness H_c so that $H|_L = H_c$ gives

$$H^{\min} = \min[c|\boldsymbol{u}|^2\sin^2(\alpha-\theta), H_c]. \tag{6.7}$$

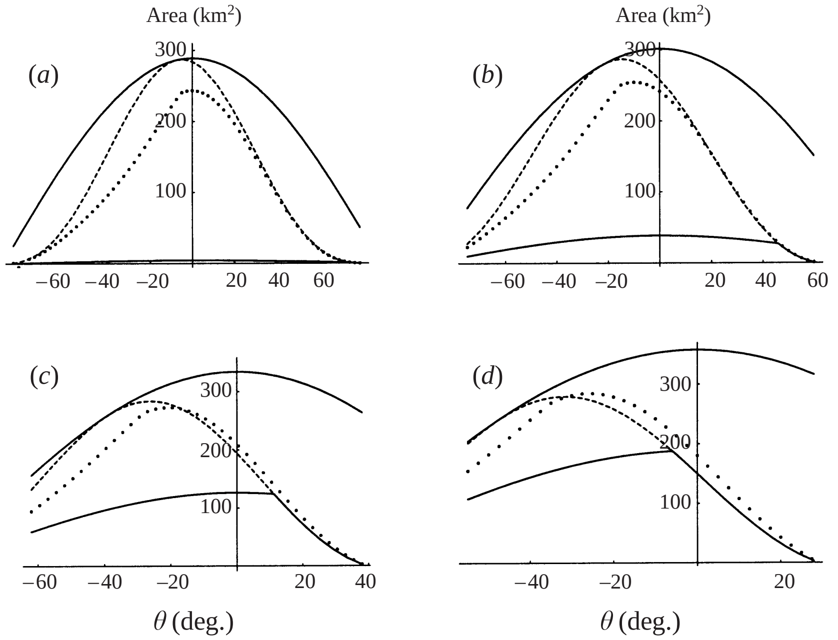

FIGURE 10. Plots of A_T (dotted line) for an idealized island of length $D = 25\,\mathrm{km}$, for varying direction of consolidated new ice drift θ, and the angle between the direction of frazil ice drift and θ equal to (*a*) 5°, (*b*) 15°, (*c*) 28°, and (*d*) 35°. Here $|\boldsymbol{U}| = 0.3\,\mathrm{m\,s^{-1}}$, $|\boldsymbol{u}| = 2|\boldsymbol{U}|$, and $F = 0.27\,\mathrm{m\,day^{-1}}$. The continuous lines represent the lower and upper bounds $DH^{\min}U/F$ and $DH^{\max}U/F$, and the dashed line represents the area of the H-constant polynya $A_T^{(c)}$.

From (6.5), the area of the polynya then satisfies

$$DH^{\min}U/F \leqslant A_T \leqslant DH^{\max}U/F. \tag{6.8}$$

Numerical experiments show that these bounds are, unfortunately, rarely tight. However, notice that if $H^{\min} = H_c$, which occurs when

$$|\boldsymbol{u}|\cos(2\alpha - \theta) < |\boldsymbol{U}|\cos\alpha, \tag{6.9}$$

then the area of the polynya, A_T, exceeds the H-constant polynya area, $A_T^{(c)}$. For example, with $\alpha - \theta = 28°$ and $|\boldsymbol{U}|/|\boldsymbol{u}| = 0.5$, inequality (6.9) shows that $A_T \geqslant A_T^{(c)}$ when $\alpha \gtrsim 39°$. More generally, $A_T \geqslant A_T^{(c)}$ if the inequality $\alpha > \alpha_{\mathrm{crit}}$ is satisfied, where α_{crit} is the solution of $|\boldsymbol{u}|\cos(2\alpha_{\mathrm{crit}} - \theta) = |\boldsymbol{U}|\cos\alpha_{\mathrm{crit}}$ lying in the range $(0°, 90°)$. When $D = 25\,\mathrm{km}$, figure 10 shows plots of A_T with varying direction of consolidated new ice drift, θ, when the angle between the direction of frazil ice drift and θ is equal to (*a*) 5°; (*b*) 15°; (*c*) 28°; (*d*) 35°. As in previous plots $|\boldsymbol{U}| = 0.3\,\mathrm{m\,s^{-1}}$, $|\boldsymbol{u}| = 2|\boldsymbol{U}|$, and $F = 0.27\,\mathrm{m\,day^{-1}}$. Also shown are the upper and lower bounds on the polynya area, $DH^{\max}U/F$ and $DH^{\min}U/F$ respectively, and the area contained by the H-constant polynya edge, $A_T^{(c)}$. Notice that in all cases the difference between A_T and $A_T^{(c)}$ is relatively small, and that the bounds on the polynya area are, in general, not tight. When the angle between the directions of drift of frazil ice and consolidated new ice, $(\alpha - \theta)$, is small ($\approx$ 5°–20°), the new polynya area is less than $A_T^{(c)}$. For larger values of $(\alpha - \theta)$ ($\approx$ 25°–40°), $A_T \geqslant A_T^{(c)}$. Notice also that the condition for $A_T \geqslant A_T^{(c)}$ found above, namely that $\alpha > \alpha_{\mathrm{crit}}$, is not a *necessary* condition, but only a sufficient condition. Referring to the example considered above, when $\alpha - \theta = 28°$, it

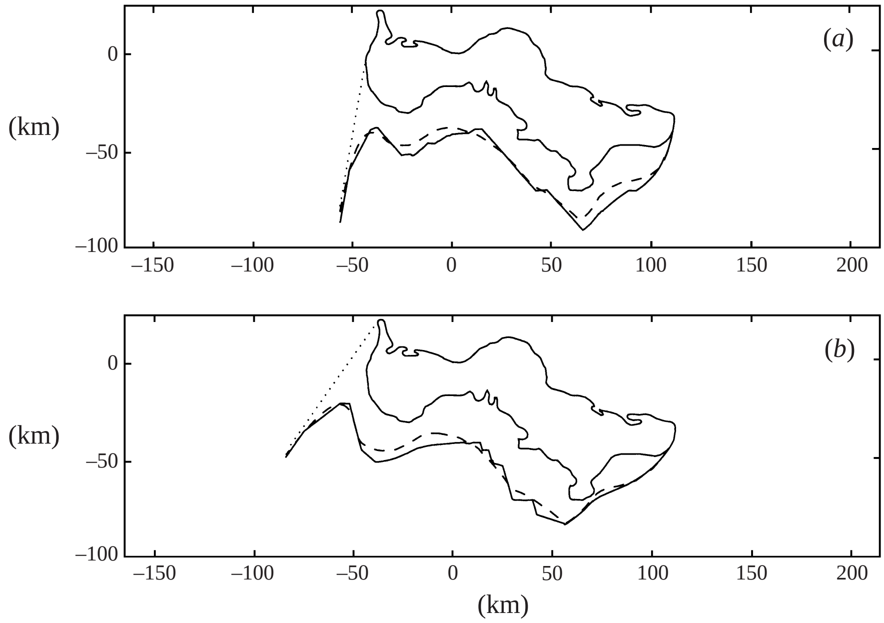

FIGURE 11. Numerical new and H-constant polynya edge solutions (solid line and dashed line, respectively), for the St. Lawrence Island Polynya when $|\boldsymbol{U}| = 0.4\,\mathrm{m\,s^{-1}}$, $|\boldsymbol{u}| = 0.8\,\mathrm{m\,s^{-1}}$, and $F = 0.27\,\mathrm{m\,day^{-1}}$. The dotted line represents the boundary of the consolidated new ice pack. In (a), $\alpha = 18°$, $\theta = -10°$ and $H_c = 0.15\,\mathrm{m}$; in (b), $\alpha = -7°$, $\theta = -35°$ and $H_c = 0.17\,\mathrm{m}$, where the vertical axis is aligned north–south, and all angles are measured positive in the counterclockwise direction from the southern axis. The axes origin is at 63.6°N, 171°W.

is sufficient for $\alpha > \alpha_{\mathrm{crit}} \approx 39°$, and thus $\theta \gtrsim 39° - 28° = 11°$, for $A_T \geqslant A_T^{(c)}$, and this is verified in figure 10(c); in fact, reference to the figure shows that $A_T \geqslant A_T^{(c)}$ for $\theta \gtrsim -19°$.

We conclude this section with a brief discussion of the simulation of the St. Lawrence Island Polynya (SLIP), in the northern Bering Sea. Figure 11 shows two simulations of the SLIP for the new collection depth law (solid line) and H-constant theory (dashed line); figure 11(a) depicts solutions for $\alpha = 18°$, $\theta = -10°$, and 11(b) for $\alpha = -7°$, $\theta = -35°$, where the vertical axis is aligned north–south, and angles are measured positive counter-clockwise from the southern axis. In both cases, $|\boldsymbol{u}| = 0.8\,\mathrm{m\,s^{-1}}$, $|\boldsymbol{U}| = 0.4\,\mathrm{m\,s^{-1}}$, and $F = 0.27\,\mathrm{m\,day^{-1}}$. The large values for the velocities are consistent with previous simulations (Darby *et al.* 1995; Morales Maqueda & Willmott 1999). The value of H_c adopted in each of the H-constant plots is simply the average of the varying H along the extent of the corresponding new polynya edges; this gives $H_c = 0.15\,\mathrm{m}$ in figure 11(a), and $H_c = 0.17\,\mathrm{m}$ in figure 11(b). In both cases, the new polynya edges show good agreement with their H-constant counterparts, although it is interesting to note the many corners which appear in the new edge. Their occurrence is not altogether surprising, since even for the simple coastline geometries examined earlier, the associated polynya edge displayed at least one corner along its length, showing that the new collection depth law is extremely sensitive to depth of the frazil ice reaching the polynya edge. Using realistic coastlines, it is possible that a frazil ice trajectory emanating from the coast intersects the coastline for a second time. In this case, the enclosed region bounded by the trajectory and the coastline is assumed to be covered in land-fast ice. These regions clearly produce step-discontinuities in the depth of frazil ice reaching the polynya edge, which contribute to the non-smooth nature of the solution. Smoothing of the island coastline will reduce the magnitude of these step-discontinuities, and produce a polynya edge with correspondingly fewer corners.

7. Summary and concluding remarks

Previous polynya flux models have specified a constant value for the collection depth, H, of consolidated new ice at the edge of a polynya. A disadvantage of this approach is that it is possible for the frazil ice thickness within the polynya to exceed H in unsteady two-dimensional polynya flux models, thereby violating a key assumption in the derivation of the ice flux balance at the polynya edge. Clearly H is a quantity which should be determined from an analysis of the physics which describes the conversion of frazil ice to consolidated new ice at the polynya edge. This paper derives a parameterization for H which is similar to that obtained for the pile-up depth of grease ice in a lead by Bauer & Martin (1983). The parameterization for H is based on the idea that the horizontal gradient of the depth-integrated momentum flux balances the frazil ice set-up when viewed in a frame of reference which moves with the velocity of the consolidated new ice. In two dimensions, the parameterization takes the form $H = h_C + c|(\boldsymbol{u} - \boldsymbol{U}) \cdot \boldsymbol{n}|^2$, where h_C is the depth of frazil ice at the polynya edge $\mathscr{C}$, $\boldsymbol{n}$ is a unit normal to the curve $\mathscr{C}$, $\boldsymbol{u} - \boldsymbol{U}$ is the relative velocity of the frazil ice with respect to the consolidated new ice region, and c is a constant whose value is tightly constrained, namely $c \approx 0.665\,\mathrm{m}^{-1}\,\mathrm{s}^2$. Clearly, $H > h_C$, and therefore flux models which adopt this parameterization for H are robust.

The unsteady one-dimensional problem for the opening of a polynya which incorporates the new parameterization of H is studied, and the results are compared with the H-constant theory (Ou 1988; Morales Maqueda & Willmott 1999). The polynya edge is found to evolve more slowly to its steady-state width than the H-constant solution. Further, when the speeds of frazil ice drift (u) and consolidated new ice drift (U) satisfy $U/u \approx 0.6$, this discrepancy in the rate of evolution can, during the spin-up, lead to significant differences (up to 13% of the final steady-state width) in the position of the new and H-constant edges. We anticipate that the time-dependent adjustment of a two-dimensional polynya to changes in the wind stress, for example, will also differ significantly from the H-constant theory discussed by Morales Maqueda & Willmott (1999).

Within the one-dimensional framework, the effect of varying the air temperature and offshore wind speed on the steady-state width and spin-up time for the polynya flux model is also examined, and compared with the corresponding H-constant results. The steady-state width grows quadratically with increasing wind speeds in contrast with the approximate lack of variation (for wind speeds greater than about $10\,\mathrm{m\,s}^{-1}$) exhibited by the H-constant steady-state width. As a consequence, the spin-up time to the steady-state width increases linearly with increasing wind speed, compared to a corresponding decrease in the H-constant spin-up time. The changes in steady-state width and spin-up time due to variations in air temperature are similar to those exhibited by the H-constant theory: an increase in air temperature produces an increase in both these quantities.

The structure of steady-state polynyas formed on the lee side of semi-infinite and finite-length straight coastal barriers are also studied, using the new parameterization for H. Qualitatively, the polynya edge solutions are similar to those which arise from assuming a constant frazil ice collection depth. However, for polynyas adjacent to both of these coastline configurations, the edges can, in certain circumstances, exhibit a corner at the point where the equilibrium width is reached. To be precise, if θ and γ denote the angles (measured positive in a counterclockwise sense) made by the consolidated new ice velocity $\boldsymbol{U}$ and the relative velocity $\boldsymbol{u} - \boldsymbol{U}$ with the offshore coordinate axis, respectively, a corner will occur when $\theta + \gamma > 0$. This is a consequence of the new parameterization for H, since it is found that for given values of θ and γ, h_C is bounded above by $h_C^{\max}(\theta, \gamma)$. When $\theta + \gamma > 0$, the only possible polynya edge solution which satisfies $h_C < h_C^{\max}(\theta, \gamma)$ for all points on $\mathscr{C}$ is one in which a corner occurs.

The new parameterization for H also has important consequences for the alongshore adjustment length scale L^a, which controls how responsive the steady-state polynya edge is to perturbations in the coastline profile. A perturbation in the coastline shape induces a perturbation in the polynya edge. It is found that L^a provides an e-folding length scale for the perturbed polynya edge in an alongshore direction which is dependent upon the sign of $\theta + \gamma$. When $\theta + \gamma = 0$, the polynya edge reproduces the perturbed coastline shape precisely.

The area of a polynya, A_T, supported by a finite-length straight coastal barrier, which can be considered as a prototype island, is also considered. The new parameterization for H leads to a complicated expression for A_T, which is not amenable to analysis. Instead, bounds on A_T are derived, based on the fact that upper and lower bounds for H can be obtained. It is found that $A_T \geqslant A_T^{(c)}$, the area of the polynya associated with a constant value for H, for a relatively large range of α (the angle, measured positive in a counterclockwise sense, between the frazil ice velocity $\boldsymbol{u}$ and the offshore coordinate axis) and θ.

Two simulations of the St. Lawrence Island Polynya (SLIP) are also presented, both with the new collection depth law for consolidated new ice, and, for comparison, with a constant value for the collection depth obtained by averaging the value of H along the new edge. Both comparisons result in good agreement between the two solutions.

Polynya edge solutions found with the new parameterization of the frazil ice collection depth H prove both qualitatively and quantitatively extremely similar to those found in the H-constant theory where a constant value for H is used. The only notable difference between the results of the two approaches is the occurrence, in certain circumstances, of a discontinuity in the gradient of the new polynya edge. The new frazil ice collection depth law provides a viable alternative to taking a constant value for H, particularly in view of the fact that now $H > h_C$, and the flux modelling approach therefore becomes robust. The effect of including the new parameterization for H in an unsteady two-dimensional polynya flux model is an important topic for future investigation.

To date, polynya flux models do not take into account possible feedback processes between the atmosphere and the polynya. For example, the large ocean to atmosphere heat flux over a polynya could force mesoscale atmospheric circulations (Dethleff 1994; Lynch *et al.* 1997; Timmermann, Lemke & Kottmeier 1999), which, in turn, could modify the surface wind stress and hence the frazil ice trajectories. Polynya–ocean interactions are crucial in the formation of dense water on the Arctic and Antarctic continental shelves. Chapman & Gawarkiewicz (1997) examine deep water production in a steady coastal polynya, while Chapman (1999) develops a model for deep water formation beneath a coastal polynya whose size and surface buoyancy flux vary in time. However, in this latter study, the one-dimensional Pease (1987) model is used to determine the polynya extent, rather than the two-dimensional unsteady flux model of Morales Maqueda & Willmott (1999).

A further aspect of polynya–ocean interaction which has been overlooked is the following. Changes in the ocean surface salinity caused by brine rejection associated with frazil ice formation will force a baroclinic circulation, which in turn will modify the frazil ice motion. Frazil ice motion may also be modified by Langmuir circulations, as pointed out by Smith *et al.* (1990). To date, no coupled ocean–polynya flux model incorporates Langmuir circulations, and we suggest that this problem should be addressed.

We thank Mr A. Looms for his assistance in the preparation of some of the figures. We are also grateful to the three anonymous referees for suggestions that helped to improve the final version of this paper. N. R. T. Biggs acknowledges support from research grant GR3/11286 of the UK Natural Environment Research Council awarded to A. J. Willmott. M. A. Morales Maqueda acknowledges support from a research grant awarded to A. J. Willmott and M. S. Darby, via the 4^{th} round of the Antarctic Special Topic awards administered by the British Antarctic Survey on behalf of the UK NERC.

REFERENCES

Bauer, J. & Martin, S. 1983 A model of grease ice growth in small leads. *J. Geophys. Res.* **88**, 2917–2925.

Chapman, D. C. 1999 Dense water formation beneath a time-dependent coastal polynya. *J. Phys. Oceanogr.* **29**, 807–820.

Chapman, D. C. & Gawarkiewicz, G. 1997 Shallow convection and buoyancy equilibration in an idealized coastal polynya. *J. Phys. Oceanogr.* **27**, 555–566.

Darby, M. S., Willmott, A. J. & Mysak, L. A. 1994 A nonlinear steady-state model of the North Water Polynya, Baffin Bay. *J. Phys. Oceanogr.* **24**, 1011–1020.

Darby, M. S., Willmott, A. J. & Somerville, T. 1995 On the influence of coastline orientation on the steady-state width of a latent heat polynya. *J. Geophys. Res.* **100**, 13625–13633.

Dethleff, D. 1994 Polynyas as a possible source for enigmatic Bennet Island atmospheric plumes. In *The Polar Oceans and Their Role in Shaping the Global Environment*. Geophysical Monograph 85. American Geophysical Union.

Fichefet, T. & Goosse, H. 1998 A numerical investigation of the Ross Sea. *Ann. Geophysicae* **16**, Supplement II, C 580.

Gordon, A. L. & Comiso, J. C. 1988 Polynyas in the Southern Ocean. *Sci. Am.*, June, 70–77.

Grumbine, R. W. 1991 A model of the formation of high-salinity shelf water on polar continental shelves. *J. Geophys. Res.* **96**, 22049–22062.

Lebedev, V. L. 1968 Maximum size of a wind-generated lead during sea freezing. *Oceanol.* **8**, 313–318.

Lynch, A. H., Gluek, M. F., Chapman, W. L., Bailey, D. A. & Walsh, J. E. 1997 Satellite observation and climate system model simulation of the St. Lawrence Island Polynya. *Tellus* **49** A, 277–297.

Markus, T. & Burns, B. A. 1995 A method to estimate subpixel-scale coastal polynyas with satellite passive microwave data. *J. Geophys. Res.* **100**, 4473–4487.

Martin, S. 1981 Frazil ice in rivers and oceans. *Ann. Rev. Fluid Mech.* **13**, 379–397.

Martin, S. & Kauffman, P. 1981 A field and laboratory study of wave damping by grease ice. *J. Glaciol.* **27**, 283–313.

Morales Maqueda, M. A. & Willmott, A. J. 1999 A two-dimensional time-dependent model of a wind-driven coastal polynya: application to the St. Lawrence Island Polynya. *J. Phys. Oceanogr.* (to appear).

Ou, H. W. 1988 A time-dependent model of a coastal polynya. *J. Phys. Oceanogr.* **18**, 584–590.

Pease, C. H. 1987 The size of wind-driven coastal polynyas. *J. Geophys. Res.* **92**, 7049–7059.

Smith, S. D., Muench, R. D. & Pease, C. H. 1990 Polynyas and leads: an overview of physical processes and environment. *J. Geophys. Res.* **95**, 9461–9479.

Timmermann, R., Lemke, P. & Kottmeier, C. 1999 Formation and maintenance of a polynya in the Weddell Sea. *J. Phys. Oceanogr.* **29**, 1251–1264.

Willmott, A. J., Morales Maqueda, M. A. & Darby, M. S. 1997 A model for the influence of winds and oceanic currents on the size of a steady-state latent heat coastal polynya. *J. Phys. Oceanogr.* **27**, 2256–2275.